Effects of the symmetry energy on the isovector properties of neutron-rich nuclei within a Thomas-Fermi approach

M. C. Papazoglou and Ch. C. Moustakidis
Department of Theoretical Physics, Aristotle University of Thessaloniki, 54124 Thessaloniki, Greece
(Received 4 March 2014; revised manuscript received 2 June 2014; published 11 July 2014)

We employ a variational method, in the framework of the Thomas-Fermi approximation, to study the effect of the symmetry energy on the neutron skin thickness and the symmetry energy coefficients of various neutron-rich nuclei. We concentrate our interest on ^{208}Pb, ^{124}Sn, ^{90}Zr, and ^{48}Ca, although the method can be applied in the totality of medium and heavy neutron-rich nuclei. Our approach has the advantage that the isospin asymmetry function $\alpha(r)$, which is the key quantity for calculating isovector properties of various nuclei, is directly related to the symmetry energy as a consequence of the variational principle. Moreover, the Coulomb interaction is included in a self-consistent way and its effects can be separated easily from the nucleon-nucleon interaction. We confirm, both qualitatively and quantitatively, the strong dependence of the symmetry energy on the various isovector properties for the relevant nuclei, using possible constraints between the slope and the value of the symmetry energy at the saturation density.

DOI: 10.1103/PhysRevC.90.014305 PACS number(s): 21.65.Ef, 21.65.Mn, 21.65.Cd, 21.10.Gv

I. INTRODUCTION

Nuclear symmetry energy (SE) is the basic regulator of the isospin properties of neutron-rich nuclei [1–8]. It is expected to affect the neutron skin thickness, the coefficient of the asymmetry energy in the Bethe-Weizsacker formula, etc. In addition, the density dependence of the SE is the main ingredient of the equation of state of neutron-rich nuclear matter. Actually, there are a variety of neutron star properties that are sensitive to SE (e.g., the maximum mass value and the corresponding radius, the onset of the direct Urca process, and the crust-core transition density and pressure [2,9]).

Recently, there has been an extended theoretical [10–62] and experimental [63–73] interest in constraining the slope of the symmetry energy L close to the value of the saturation density ρ_0 of nuclear matter. Both theoretical and experimental efforts are focused on the study of a possible correlation of L with various nuclear properties, including the neutron skin thickness, the dipole polarizability, and the pygmy dipole resonance of various neutron-rich nuclei as well as the analysis of heavy-ion collision data. Additionally, isobaric analog states, nuclei mass formula data, and also neutron star observation data have also been elaborated.

However, the experimental data for the SE still remain limited and only for low values of density ($\rho < \rho_0$) are they accurately constrained. From the theoretical point of view there is an effort to constrain the trend of SE, even for low values of density, from finite nuclei properties and to extrapolate in a way to densities related to the neutron star equation of state (up to $\simeq 5\rho_0$). In any case, the constraints on L or in general the density dependence of SE, even for low values of ρ, are very important for astrophysical applications. For example, the transition density and pressure between the crust and the core in a neutron star are expected to lie close to the half values of the saturation density ρ_0 and consequently are similar to the finite nuclei interior densities [2–5].

The structure of a heavy nucleus is a result of the interplay between the strong short-range nuclear forces and long-range Coulomb interaction. However, in order to exhibit the isovector character of nuclear forces, we have to focus mainly on heavy and additional neutron-rich nuclei. Furthermore, it is well known that the energy density formalism is able to reproduce properties of finite nuclei including mainly the bulk properties, namely, the binding energy as well as the size and shape of the mass and charge distributions [50,74–78]. The Thomas-Fermi model, which has been applied previously with success for the study of the main properties of heavy nuclei, is the main framework of the present study. More precisely, we employ a variational approach, based on the Thomas-Fermi approximation, by suitably constructing an energy density functional and solving the derived Euler-Lagrange equation. Special attention is devoted to the contribution of the nuclear symmetry energy and the self-consistent treatment of the Coulomb interaction. The symmetry energy is suitably parametrized. Actually, the present approach can be easily extended to include more complicated expressions for the symmetry energy as well as for the energy of symmetric nuclear matter.

The key quantity of the present study is the isospin asymmetry function $\alpha(r) = [\rho_n(r) - \rho_p(r)]/\rho(r)$ (where ρ_n, ρ_p, and $\rho = \rho_n + \rho_p$ are the neutron, proton, and total number densities, respectively). The method has the advantage that the asymmetry function $\alpha(r)$ is directly related to the symmetry energy as a consequence of the variational principle. It is expected that the various isovector properties of nuclei (neutron skin thickness, symmetry energy coefficient, etc.) depend on the trend of the symmetry energy for densities close to the interior of the nucleus. The motivation of the present work is twofold. First, we tried to construct a self-consistent and easily applicable density functional method to study the effect of the symmetry energy on the isovector structure properties of medium and heavy neutron-rich nuclei. Second, our aim is, if possible, to combine our theoretical estimation with the relevant experimental or empirical data in order to suggest constraints on the density dependence of the symmetry energy for densities close to those of the interior of finite nuclei.

The article is organized as follows. In Sec. II we review the density functional method and the variational approach employed for calculating the bulk properties of various neutron-rich nuclei. The results are presented and discussed in Sec. III, while Sec. IV summarizes the present study.

II. ENERGY DENSITY FUNCTIONAL AND VARIATIONAL APPROACH

According to the empirical Bethe-Weizsacker formula the binding energy of a finite nucleus with A nucleons and atomic number Z is given by

$$B(A,Z) = -a_V A + a_S A^{2/3} + a_C \frac{Z(Z-1)}{A^{1/3}} + a_A \frac{(N-Z)^2}{A} + \Delta E_{\rm mic}. \quad (1)$$

The first term corresponds to the volume effect, the second is the surface term, the third one takes into account the Coulomb repulsion of the protons, while the fourth is the symmetry energy term. Finally, the last term corresponds to other factors including the pairing interaction. Using fits of known masses to this equation one can determine the corresponding coefficients a_V, a_S, a_C, and a_A.

The energy density functional is a natural extension of the above formula, where now the total energy is a functional of the proton and neutron densities and consists of terms corresponding with those appearing in relation (1). The minimization of the total energy defines the related densities and consequently the contribution of each term separately. In the present work we apply the energy density formalism, where the total energy of finite nuclei is a functional of the total density $\rho(r)$ and the isospin asymmetry function $\alpha(r)$, that is,

$$E[\rho(r),\alpha(r)] = \int_{\mathcal{V}} \mathcal{E}(\rho(r),\alpha(r))d^3r, \quad (2)$$

where $\mathcal{E}(r)$ is the local energy density. The integration is performed over the total volume $\mathcal{V}$ occupied by the relevant nuclei.

Now we consider the functional

$$E[\rho,\alpha] = \int_{\mathcal{V}} \left[\epsilon_{ANM}(\rho(r),\alpha(r)) + F_0|\nabla\rho(r)|^2 + \frac{1}{4}\rho(1-\alpha)V_c(r) \right] d^3r. \quad (3)$$

The first ingredient of the functional, $\epsilon_{ANM}(\rho(r),\alpha(r))$, corresponds to the energy density of the asymmetric nuclear matter given by the expression

$$\epsilon_{ANM}(\rho,\alpha) = \epsilon_{SNM}(\rho) + \alpha^2 \rho S(\rho), \quad (4)$$

where $\epsilon_{SNM}(\rho,\alpha)$ is the energy density of symmetric nuclear matter and $S(\rho)$ is the symmetry energy per particle of nuclear matter.

The second term $F_0|\nabla\rho(r)|^2$ is the gradient term corresponding to the contribution originating from the finite-size character of the density distribution with F_0 being a parameter in the interval (66–72) MeV. In the present work we consider that $F_0 = 70$ MeV.

The third term corresponds to the Coulomb energy density, where the Coulomb potential $V_c(r)$ is defined as

$$V_c(r) = \frac{e^2}{2} \int \frac{\rho(r')[1-\alpha(r')]}{|\mathbf{r}-\mathbf{r}'|} d^3r', \quad (5)$$

and must satisfy also the Poisson equation

$$\nabla^2 V_c(r) = 4\pi e^2 \left(\tfrac{1}{2}[1-\alpha(r)]\right)\rho(r). \quad (6)$$

Equation (6) is used to check the convergence of the iteration process involved in such calculations. Finally, the density $\rho(r)$ and the asymmetry function $\alpha(r)$ must obey the following constraints:

$$\int \rho(r)d^3r = A, \quad \int \alpha(r)\rho(r)d^3r = N - Z. \quad (7)$$

The functional (3) and the constraints (7) after some algebra are written as

$$E[\rho,\alpha] = 4\pi \int_0^\infty r^2 \left[\epsilon_{ANM}(\rho(r),\alpha(r)) + F_0 \left(\frac{d\rho}{dr}\right)^2 + \frac{1}{4}\rho(1-\alpha)V_c(r) \right] dr \quad (8)$$

and

$$4\pi \int_0^\infty r^2\rho(r)dr = A, \quad 4\pi \int_0^\infty r^2\alpha(r)\rho(r)dr = N - Z. \quad (9)$$

Equations (8) and (9) constitute a variational problem with constraints while the Lagrangian density is given by

$$\mathcal{L} = 4\pi r^2 \left(\epsilon_{ANM}(\rho,\alpha) + F_0 \left(\frac{d\rho}{dr}\right)^2 + \frac{1}{4}\rho(1-\alpha)V_c(r) \right) - \lambda_1 4\pi r^2\rho - \lambda_2 4\pi r^2\alpha\rho. \quad (10)$$

In Eq. (10) λ_1 and λ_2 are the Lagrange multipliers. The two corresponding Euler-Lagrange equations for $\rho(r)$ and $\alpha(r)$ are defined as follows:

$$\frac{\partial\mathcal{L}}{\partial\rho} - \frac{d}{dr}\left(\frac{\partial\mathcal{L}}{\partial\rho'}\right) = 0, \quad (11)$$

$$\frac{\partial\mathcal{L}}{\partial\alpha} - \frac{d}{dr}\left(\frac{\partial\mathcal{L}}{\partial\alpha'}\right) = 0. \quad (12)$$

We find easily that

$$\frac{\partial\mathcal{L}}{\partial\rho} = 4\pi r^2 \left[\frac{\partial\epsilon_{SNM}(\rho)}{\partial\rho} + \alpha^2 \left(S(\rho) + \rho\frac{\partial S(\rho)}{\partial\rho} \right) + \frac{1}{4}(1-\alpha)V_c(r) - \lambda_1 - \lambda_2\alpha \right], \quad (13)$$

$$\frac{\partial\mathcal{L}}{\partial\rho'} = 8\pi r^2 F_0\rho', \quad (14)$$

$$\frac{d}{dr}\left(\frac{\partial\mathcal{L}}{\partial\rho'}\right) = 8\pi F_0 r^2\rho'' + 16\pi F_0\rho' r. \quad (15)$$

Also we have

$$\frac{\partial \mathcal{L}}{\partial \alpha} = 4\pi r^2 \left[2\alpha\rho S(\rho) - \frac{1}{4}\rho V_c(r) - \lambda_2 \rho \right], \quad (16)$$

$$\left(\frac{\partial \mathcal{L}}{\partial \alpha'} \right) = 0. \quad (17)$$

The first Euler-Lagrange equation gives

$$\rho'' + \frac{2\rho'}{r} - \frac{1}{2F_0}\left[\frac{\partial \epsilon_{SNM}(\rho)}{\partial \rho} + \alpha^2 \left(S(\rho) + \rho \frac{\partial S(\rho)}{\partial \rho} \right) + \frac{1}{4}(1-\alpha)V_c(r) - \lambda_1 - \lambda_2 \alpha \right] = 0 \quad (18)$$

and the second one gives

$$\alpha(r) = \frac{V_c(r)}{8S(\rho)} + \frac{\lambda_2}{2S(\rho)} = \frac{1}{8S(\rho)}(V_c(r) + 4\lambda_2). \quad (19)$$

The asymmetry function $\alpha(r)$ obeys the constraints $0 \leqslant \alpha(r) \leqslant 1$. However, expression (19) does not ensure the above constraints, since for high values of r [low values of $\rho(r)$ and consequently $S(\rho)$] $\alpha(r)$ increases very fast and there is a cutoff radius r_c, where $\alpha(r_c) = 1$ and also $\alpha(r \geqslant r_c) \geqslant 1$.

In order to overcome this unphysical behavior of $\alpha(r)$ we use the assumption

$$\alpha(r) = \begin{cases} \frac{1}{8S(\rho)}[V_c(r) + 4\lambda_2], & r \leqslant r_c \\ 1, & r \geqslant r_c. \end{cases} \quad (20)$$

Accordingly, the proton and neutron density distributions take the form

$$\rho_p(r) = \begin{cases} \frac{1}{2}\rho(r)[1-\alpha(r)], & r \leqslant r_c, \\ 0, & r \geqslant r_c. \end{cases} \quad (21)$$

$$\rho_n(r) = \begin{cases} \frac{1}{2}\rho(r)[1+\alpha(r)], & r \leqslant r_c, \\ \rho(r), & r \geqslant r_c. \end{cases} \quad (22)$$

The Lagrange multiplier λ_2 is found from the normalization condition

$$\int_{\mathcal{V}} \alpha(r)\rho(r) d^3r = N - Z, \quad (23)$$

where the integration is performed over the total volume occupied by the specific nucleus by considering that $\alpha(r)$ is given by (20). After straightforward algebra we get

$$\lambda_2 = 2\left(\int_{\mathcal{V}_c} \rho(r) d^3r - \frac{e^2}{8} \int_{\mathcal{V}_c} \frac{V_c(r)\rho(r)}{S(\rho)} d^3r - 2Z \right) \times \left(\int_{\mathcal{V}_c} \frac{\rho(r)}{S(\rho)} d^3r \right)^{-1}, \quad (24)$$

where $\mathcal{V}_c$ is the part of the spherical volume of the nucleus for the radius r_c. The cutoff radius r_c, which reflects the combined effect of the symmetry energy and Coulomb energy on the asymmetry function $\alpha(r)$ according to expression (19), easily can be determined by solving the equation

$$\alpha(r_c) = 1. \quad (25)$$

Finally, from Eqs. (20), (24), and (25) we see that the asymmetry function $\alpha(r)$ is

$$\alpha(r) = \frac{1}{S(\rho)} \left(\frac{V_c(r) - V_c(r_c)}{8} + S(\rho_c) \right), \quad r \leqslant r_c, \quad (26)$$

and $\alpha(r) = 1$ for $r \geqslant r_c$. In Eq. (26) one can see clearly exhibited the interplay between the long-range Coulomb interaction and the short-range isovector part of the nuclear forces. Actually, $S(\rho)$ affects $\alpha(r)$ in a twofold manner: (a) directly via the term $S(\rho_c)/S(\rho)$ and (b) indirectly since $V_c(r)$ according to Eq. (5) is a functional of $\alpha(r)$. In the simplified case where $V_c(r)$ is excluded, the asymmetry function is given by the simple formula

$$\alpha(r) = \frac{S(\rho_c)}{S(\rho)}. \quad (27)$$

The Coulomb potential, given by Eq. (5) due to the discontinuity behavior of the proton density distribution [Eq. (21)], is decomposed into two parts as follows:

$$V_c^A(r) = 2\pi e^2 \left[\frac{1}{r} \int_0^r [1-\alpha(r')]\rho(r') r'^2 dr' + \int_r^{r_c} [1-\alpha(r')]\rho(r') r' dr' \right], \quad r \leqslant r_c, \quad (28)$$

$$V_c^B(r) = \frac{2\pi e^2}{r} \int_0^{r_c} [1-\alpha(r')]\rho(r') r'^2 dr', \quad r \geqslant r_c. \quad (29)$$

Actually, one has to solve self-consistently Eqs. (18) and (19) with the corresponding constraints (9). In the present work, in order to avoid the complication due to the differential equation (18) we employ a variational method where use is made of an appropriate trial function for $\rho(r)$. This method, as pointed out by Brueckner *et al.* [79–82] and Lombard [83], provides a convenient tool in seeking an approximate solution for heavy nuclei. There are a variety of trial density distribution functions suitably parametrized to describe light, medium, and heavy nuclei. In the present study we consider the trial function given by the Fermi-type formula

$$\rho(r) = \frac{n_0}{1 + \exp[(r-d)/w]}. \quad (30)$$

In addition, for the basic ingredients of the energy functional (8) we consider a model where the energy of symmetric nuclear matter is given by [84]

$$\epsilon_{SNM}(\rho) = \rho T_o(au^{2/3} - bu + cu^{5/3}), \quad u = \rho/\rho_0, \quad (31)$$

where $T_o = 37.0206$ MeV and $\rho_0 = 0.16144$ fm^{-3} (the saturation density). The corresponding constants are $a = -0.08203$, $b = 0.97342$, and $c = 0.61687$.

The symmetry energy $S(\rho)$ can be suitably expanded around the saturation density ρ_0 as follows:

$$S(\rho) = S(\rho_0) + L\delta + \frac{K_{\rm sym}}{2!}\delta^2 + O(\delta^3), \quad (32)$$

where $S(\rho_0)$ is the value of the symmetry energy at the saturation density and $\delta = \frac{\rho-\rho_0}{3\rho_0}$. The coefficient $L = 3\rho_0 \frac{dS(\rho)}{d\rho}|_{\rho=\rho_0}$ is related to the slope of the symmetry energy at ρ_0, while the coefficient $K_{\rm sym}$ is given by $K_{\rm sym} = 9\rho_0^2 \frac{d^2S(\rho)}{d\rho^2}|_{\rho=\rho_0}$.

There are various suggested expressions for the symmetry energy in the literature. Here we employ the simple parametrization

$$S(\rho) = S(\rho_0)\left(\frac{\rho}{\rho_0}\right)^{\gamma} = Ju^{\gamma}, \quad S(\rho_0) = J. \tag{33}$$

Obviously, in this case the parameter γ is related to both the slope L and J by the expression

$$\gamma = \frac{L}{3J}. \tag{34}$$

It is worth pointing out that, for $\gamma < 1$, a smaller value of γ gives a stiffer $S(\rho)$ for $\rho < \rho_0$ while, for $\rho > \rho_0$, the higher the value of γ the stiffer is $S(\rho)$. Finally, the symmetry energy density $s(\rho)$ is given by

$$s(\rho) = \rho J u^{\gamma}. \tag{35}$$

Now the total energy density of the asymmetric nuclear matter is

$$\epsilon_{ANM}(\rho,\alpha) = \rho T_o(au^{2/3} - bu + cu^{5/3}) + \alpha^2 \rho J u^{\gamma}. \tag{36}$$

For each specific set of Fermi-type distribution parameters n_0, d, and w and a given symmetry energy $S(\rho)$, we calculate the asymmetry density $\alpha(r)$ and the total energy of the specific nucleus. The set of density distribution parameters is adjusted in order to find the corresponding minimum value of the total energy given now by the integrals

$$\begin{aligned} E[\rho(r);\gamma] = 4\pi \int_0^{r_c} r^2 \Bigg(& \epsilon_{ANM}(\rho(r),\alpha(r)) + F_0\left(\frac{d\rho}{dr}\right)^2 \\ & + \frac{1}{4}\rho(r)[1-\alpha(r)]V_c(r)\Bigg) dr \\ & + 4\pi \int_{r_c}^{\infty} r^2 \left(\epsilon_{ANM}(\rho(r),1) + F_0\left(\frac{d\rho}{dr}\right)^2\right) dr. \end{aligned} \tag{37}$$

After finding the density $\rho(r)$ and asymmetry function $\alpha(r)$ which minimize the total energy, all the relevant quantities are easily calculated.

One possibility is to calculate the symmetry energy coefficient a_A defined in the Bethe-Weizsacker formula via the local density approximation. In this approach a_A is defined by the integral

$$a_A = \frac{A}{(N-Z)^2} \int \rho(r) S(\rho) \alpha^2(r) d^3r. \tag{38}$$

Definition (38) shows explicitly the direct strong dependence of a_A on the symmetry energy $S(\rho)$ and the asymmetry function $\alpha(r)$. Actually, according to the present study, the total integral is split into two parts as follows:

$$\begin{aligned} a_A = \frac{A}{(N-Z)^2} \Bigg(& \int_{\mathcal{V}_c} \rho(r) S(\rho) \alpha^2(r) d^3r \\ & + \int_{\mathcal{V}>\mathcal{V}_c} \rho(r) S(\rho) d^3r \Bigg). \end{aligned} \tag{39}$$

One of the most important quantities concerning the isovector character of the nuclear forces is the neutron skin thickness defined as

$$R_{\text{skin}} = R_n - R_p, \tag{40}$$

with R_n and R_p are the neutron and proton radii, respectively, defined as

$$R_n = \left(\frac{1}{N}\int r^2 \rho_n(r) d^3r\right)^{1/2}, \quad R_p = \left(\frac{1}{Z}\int r^2 \rho_p(r) d^3r\right)^{1/2}. \tag{41}$$

In the framework of the present approach they are given, respectively, by the expressions

$$\begin{aligned} R_n = \Bigg[\frac{1}{N} \Bigg(& \int_{\mathcal{V}_c} r^2 \frac{1}{2}\rho(r)\,[1+\alpha(r)]\, d^3r \\ & + \int_{\mathcal{V}>\mathcal{V}_c} r^2 \rho(r) d^3r \Bigg)\Bigg]^{1/2} \end{aligned} \tag{42}$$

and

$$R_p = \left(\frac{1}{Z}\int_{\mathcal{V}_c} r^2 \frac{1}{2}\rho(r)\,[1-\alpha(r)]\, d^3r\right)^{1/2}. \tag{43}$$

Actually, R_{skin} is not directly dependent on $S(\rho)$, compared to the case of a_A, but indirectly dependent via the dependence of $\alpha(r)$. However, in recent studies it has been conjectured that R_{skin} is a strong indicator of the isospin character of the nuclear interaction expected to be strongly correlated with the symmetry energy slope L and the value J or in general with the values of the symmetry energy close to saturation density.

III. RESULTS AND DISCUSSION

We employ a variational approach to study the effect of the symmetry energy on isovector properties of various medium and heavy nuclei. The method, given its simplicity, has the advantage that the dependence of the asymmetry function $\alpha(r)$ on the symmetry energy and the Coulomb potential are introduced explicitly. More specifically, the total energy density of the nucleus consists of nuclear and Coulomb contributions. The nuclear term consists of two parts, i.e., symmetric nuclear matter and asymmetry energy. In order to be able to study the effects of the symmetry energy we parametrized suitably the related expression. It is noted that the results obtained in the present study are based on the assumption given in Eq. (33), where accordingly the main parameters L and J are linearly related, that is, $L = 3\gamma J$. We study the dependence of the neutron skin thickness R_{skin} and the asymmetry coefficient a_A on the slope L of the SE at the saturation density ρ_0. In the present method the asymmetry function $\alpha(r)$ is treated as a variational function and the total density $\rho(r)$ as a trial function. For each $\rho(r)$ the corresponding $\alpha(r)$ and the total energy are found. The process continues until the function ρ that minimizes the total energy is found. All the relevant quantities, which are functionals of $\rho(r)$, $\alpha(r)$, and $S(\rho)$, are easily calculated.

The outline of our approach is the following: We start from the general relation $R = r_0 A^{1/3}$, which gives an averaged estimate of the nuclear radius, and, accordingly, we consider a Fermi form for the total density distribution $\rho(r)$ [85].

Afterward, for a fixed $\rho(r)$ the asymmetry function is rearranged accordingly so that the total energy of the nucleus is the lowest one.

It is worth pointing out, following the discussion by Brueckner *et al.* [80], that the energy density functional (3) breaks down at the edge of the nucleus for two reasons. First, the Thomas-Fermi approximation, which is the basis of the present work, fails for low densities. Second, at the edge of the nucleus, the asymmetry function $\alpha(r)$ tends to unity and the potential contribution to the total energy functional is not accurate. For a recent discussion of the connection of the density functional formalism with the nuclear matter equation of state and the distinct features of the finite-size effect of nuclei see Ref. [86]. In the present work we employ a variational treatment of an energy functional, without any additional constraints, requiring just the minimization of the binding energy. That is, we do not impose any additional constraints on the functional, for example to reproduce accurately the proton radii. This approach will be suitable if we intend to impose stronger constraints on the values of L and J and might be of interest for future work. However, the main motivation of the present work is not to find the suitable energy density functional to reproduce simultaneously the experimental values of proton radii and energy but to focus on the symmetry energy effects on neutron-rich nuclei properties.

In Fig. 1, the symmetry energy versus the total density is plotted, according to Eq. (33), for various values of the slope parameter L. It is noted that lower values of L, for low values of density ($\rho < \rho_0$), correspond to higher values of $S(\rho)$. This behavior of $S(\rho)$ is well reflected in the values of the total binding energy $E_{\rm tot}$ and the asymmetry function $\alpha(r)$. More precisely, higher values of L lead to a lower contribution of $S(\rho)$ to the total binding energy and consequently the nucleons become more bound. For example, in Table I are presented the results (concerning the total binding energy $E_{\rm tot}$, the proton and neutron rms radii R_p and R_n, respectively, the neutron skin $R_{\rm skin}$, and the asymmetry coefficient a_A) for the nucleus

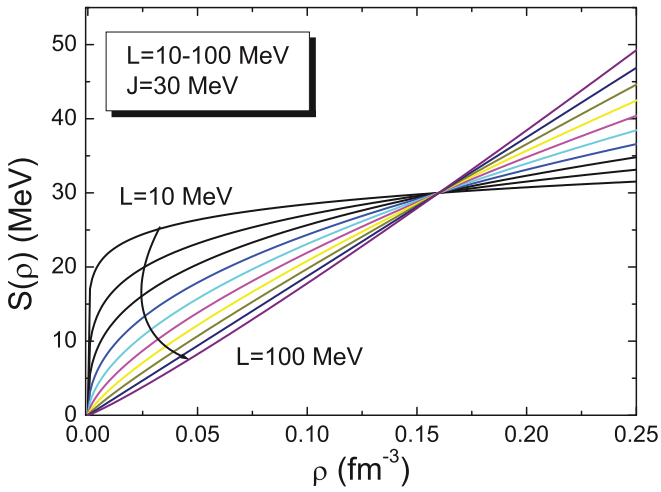

FIG. 1. (Color online) The nuclear symmetry energy $S(\rho)$, defined in Eq. (33), as a function of the density ρ for various values of the slope parameter L and the specific value $J = 30$ MeV.

TABLE I. The slope parameter L (in MeV), the binding energy E (in MeV), the neutron radius R_n (in femtometers), the proton radius R_p (in femtometers), the neutron skin thickness $R_{\rm skin}$ (in femtometers), and the asymmetry coefficient a_A (in MeV) calculated for a fixed value $J = 30$ MeV. L and J are linearly related, that is, $L = 3\gamma J$.

L	E	R_n	R_p	$R_{\rm skin}$	a_A
10	−1581.36	5.629	5.623	0.006	28.52
20	−1593.44	5.659	5.604	0.055	26.77
30	−1606.35	5.695	5.586	0.109	24.85
40	−1620.28	5.723	5.560	0.163	22.90
50	−1633.62	5.756	5.537	0.219	20.87
60	−1646.40	5.780	5.517	0.263	19.03
70	−1658.36	5.803	5.500	0.303	17.32
80	−1669.35	5.816	5.478	0.338	15.80
90	−1679.37	5.828	5.458	0.370	14.41
100	−1688.46	5.846	5.448	0.398	13.11

^{208}Pb for the case $J = 30$ MeV and for $10 \leqslant L \leqslant 100$ MeV. In addition, since the values of the density distribution inside the nucleus are lower than the value of the saturation density $\rho_0 = 0.16$ fm^{-3}, it is concluded that the isovector properties of nuclei are related to the trend of the symmetry energy in the region $0 < \rho < \rho_0$ and vice versa; that is, the experimental isovector measurements give information for the lower part of the SE.

In Fig. 2 we plot the density distributions (total, proton, and neutron) as well as the corresponding asymmetry function $\alpha(r)$ for various values of L and two nuclei (^{208}Pb and ^{48}Ca.) The softness symmetry energy (higher values of L) shifts the neutron distribution to the outer part of the nucleus, while at the same time it concentrates the protons more deeply. This is clearly reflected both on the corresponding values of R_p and R_n as well as on the neutron skin $R_{\rm skin}$ (see also Table I). The effects of the symmetry energy are even more pronounced on the trend of the asymmetry function. Higher values of L shift the cutoff radius r_c to even lower values, increasing dramatically the neutron skin and forming a kind of *neutron halo* inside the nucleus. It is obvious from the above analysis that $S(\rho)$ and consequently, according to expression (26), the asymmetry function $\alpha(r)$ act as a *regulator* on the proton and neutron distributions in order to minimize, in every case, the total energy of the nucleus. On the other hand [see also expression (26)], the Coulomb potential $V_c(r)$ acts inversely, compared to $S(\rho)$, and its main effect is to shift the proton distribution to the outer part of the nucleus. Actually, the interplay among the long-range Coulomb forces, the nuclear forces, and mainly the isovector part of nuclear forces is responsible for the creation of the neutron skin thickness. However, although the Coulomb contribution is well defined, the contribution of the symmetry energy still remains an open problem even for low values of densities.

Figure 3(a) displays the neutron skin $R_{\rm skin}$ as a function of L for various values of J for ^{208}Pb. The most striking feature is, in all cases, the strong dependence of $R_{\rm skin}$ on L. For a comparison, we include for the case of ^{208}Pb an approximate

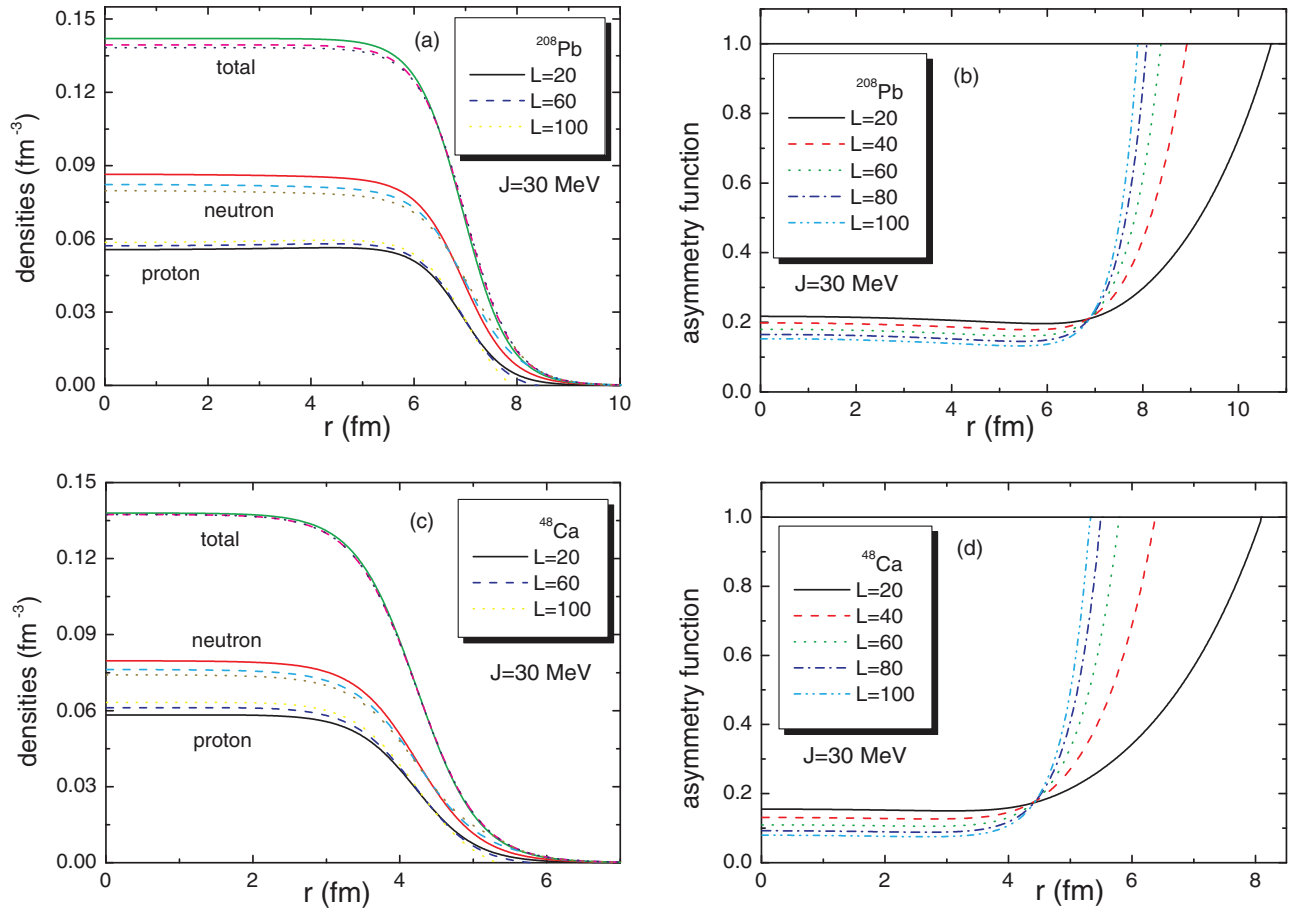

FIG. 2. (Color online) The total, neutron, and proton density distributions [(a) and (c)] for ^{208}Pb and ^{48}Ca for three values of L [(a) and (c)] and the corresponding asymmetry functions $\alpha(r)$ for a variety of values of L [(b) and (d)].

linear dependence

$$R_{\rm skin}({\rm fm}) = 0.101 + 0.00147\ L\ ({\rm MeV}), \qquad (44)$$

established by Centelles *et al.* [20] using a wide range of nonrelativistic and relativistic models. It is obvious that relation (44) supports a softer dependence of $R_{\rm skin}$ on L compared to the present study. However, we note that we present a systematic study of the effects of L on $R_{\rm skin}$ and in a large range of values of L without trying to reproduce for example the experimental value of the binding energy or the charge radius of the specific nucleus. Even in this case, we found that the intersection between our results and the results compatible with (44) corresponds to values of binding energy very close to the experimental values for the specific nuclei.

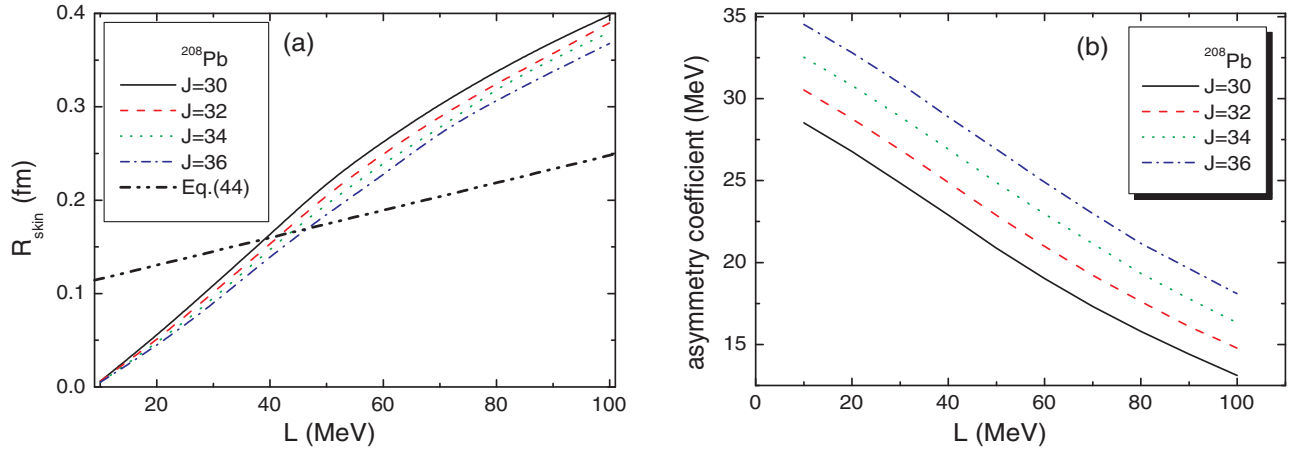

FIG. 3. (Color online) (a) The neutron skin $R_{\rm skin}$ for ^{208}Pb as a function of the symmetry energy slope L for various values of J. (b) The asymmetry coefficient a_A for ^{208}Pb as a function of the symmetry energy slope L for various values of the parameter J.

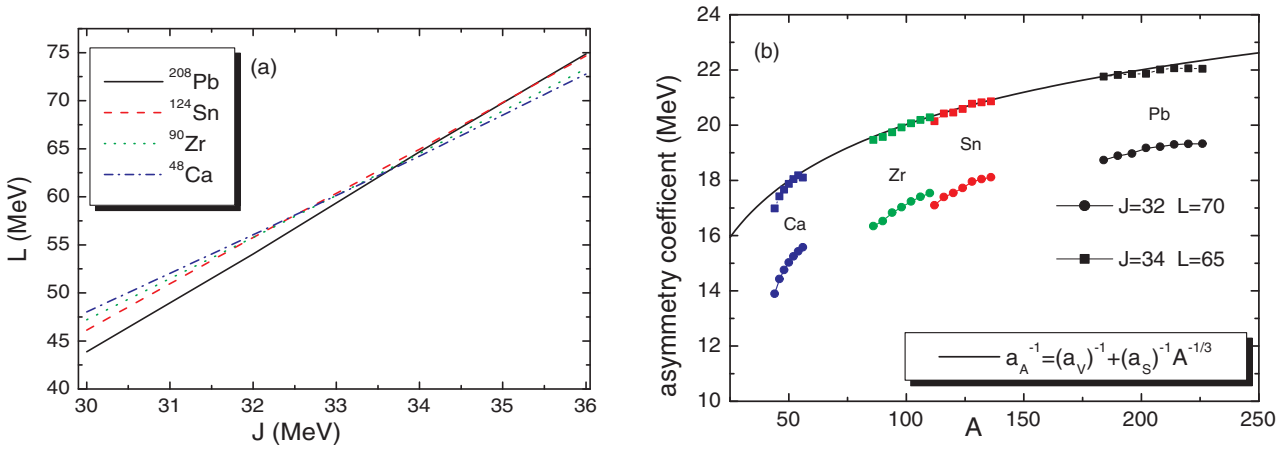

FIG. 4. (Color online) (a) Plot of the pairs L and J that reproduce the empirical value of a_A given by (45) for four nuclei. (b) The asymmetry coefficients a_A as a function of A for the relevant isotopes and for the sets $L = 70$, $J = 32$ and $L = 65$, $J = 34$. The solid line corresponds to the empirical formula (45) (for more details see text).

Very recently the Lead Radius Experiment (PREX) at the Jefferson Laboratory has provided the first model-independent evidence for the existence of a neutron-rich skin in ^{208}Pb [66,67]. The determined neutron skin was $R_{\rm skin} = 0.33^{+0.16}_{-0.18}$ fm. However, such a large error is not enough to constrain the various nuclear models. In addition, the large determined neutron skin (compared to previous experimental measurements) creates a new open problem concerning the correlation between the nuclear equation of state of nuclear matter and density functional theory in finite nuclei (see [34,57] for a pertinent discussion).

In Fig. 3(b) we display the coefficients a_A as a function of L for various values of J. It is obvious that a_A is a decreasing function of L. Actually, for specific pairs of values of N and Z, and according to the Bethe-Weizsacker formula (1), a softer $S(\rho)$ (high values of L) leads to a lower value of $\alpha(r)$ (a property directly connected with the contribution of the symmetry energy to the total energy). Obviously, a_A exhibits a mass-dependent behavior.

In order to impose some possible constraints on the values of L, we plot in Fig. 4(a) for each of the four nuclei ^{208}Pb, ^{124}Sn, ^{90}Zr, and ^{48}Ca the pairs of L and J consistent with the corresponding empirical values of a_A determined by the formula [13]

$$a_A^{-1} = (a_V)^{-1} + (a_S)^{-1}A^{-1/3}, \tag{45}$$

where we use for the volume and surface coefficients $a_V = 35.5$ MeV and $a_S = 9.9$ MeV, respectively. By combining Eqs. (19), (23), and (38) we get the expression

$$\frac{A}{a_A} = \mathcal{I}_1\left[1 + \frac{1}{64(N-Z)^2}\left(\mathcal{I}_1\mathcal{I}_3 - \mathcal{I}_2^2\right)\right]^{-1}, \tag{46}$$

where

$$\mathcal{I}_1 = \int \frac{\rho(r)}{S(\rho)}d^3r, \quad \mathcal{I}_2 = \int \frac{V_c(r)\rho(r)}{S(\rho)}d^3r,$$
$$\mathcal{I}_3 = \int \frac{V_c^2(r)\rho(r)}{S(\rho)}d^3r. \tag{47}$$

The integral $\mathcal{I}_1$ is decomposed as

$$\mathcal{I}_1 = \frac{A}{J} + \frac{1}{J}\int \rho(r)\left(\frac{J}{S(\rho)} - 1\right)d^3r. \tag{48}$$

The main contribution to the integral on the right-hand side of Eq. (48) originates mainly from the surface region [13]. By taking into account the surface contribution denoted by the coefficient Q_s, Eq. (46) finally is written as

$$\frac{A}{a_A} = \left(\frac{A}{J\,(1+\Delta_c)} + \frac{A^{2/3}}{Q_s\,(1+\Delta_c)}\right), \tag{49}$$

where Q_s is given by

$$Q_s = JA^{2/3}\left(\int \rho(r)\left(\frac{J}{S(\rho)} - 1\right)d^3r\right)^{-1}, \tag{50}$$

while the contribution due to the Coulomb interaction Δ_c is

$$\Delta_c = \frac{1}{64(N-Z)^2}\left(\mathcal{I}_1\mathcal{I}_3 - \mathcal{I}_2^2\right). \tag{51}$$

Comparing formula (45) and Eq. (49) makes it obvious that the volume coefficient a_V and the surface coefficient a_S are directly related to the value of the symmetry energy at the saturation density J and the coefficient Q_s, respectively. In the specific case where the Coulomb interaction is excluded, a_V and a_S are identified with J and Q_s, respectively [13].

It is seen in Fig. 4(a) that the set $J = 34$ MeV and $L = 65$ MeV reproduces very well the empirical values of a_A for almost all the medium and heavy isotopes.

Two important features of the relation between L and J are useful. First, the inequality $4.13 \leqslant \Delta L/\Delta J \leqslant 5.18$ holds approximately. This means that a change of 1 MeV in the value of J results in a corresponding change $4.13 \leqslant \Delta L \leqslant 5.18$ MeV. That is, according to the present approach the accuracy on the measurements of a_A and J will impose strong constraints on the values of L.

Second, since the four almost linear curves are arranged very close together and have a similar slope, we may conjecture that a possible universal dependence holds between L and J for nuclei at least in the mass region $A = 40$–200. That means that

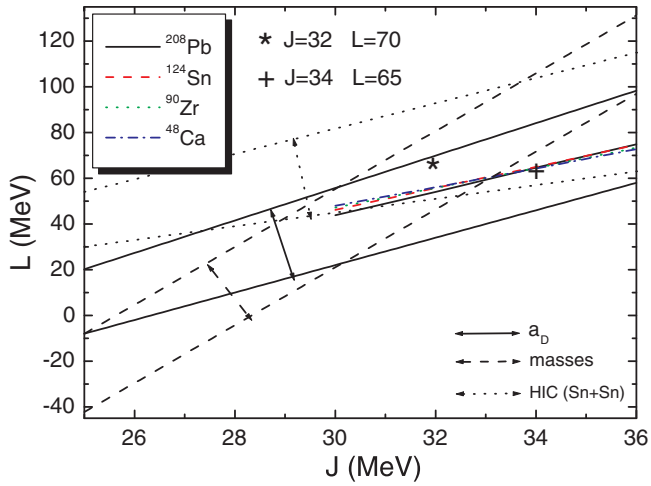

FIG. 5. (Color online) Regions of allowed values of pairs J and L (three bands) constrained from heavy-ion collisions [HIC(Sn + Sn) case] and nuclear structure observables (a_D and nuclear masses) (for more details see Ref. [10]) in comparison with the corresponding results constrained from the present approach. The solid, dashed, and dotted arrows indicate constraints related to a_D, nuclear masses, and heavy-ion collisions, respectively. The four colored lines intersecting at the cross show the dependence of L on J according to Fig. 5(a) of our present work. The star and the cross correspond to the sets $L = 70$, $J = 32$ and $L = 65$, $J = 34$, respectively (for more details see text).

the same set of L and J, related to nuclear symmetry energy, reproduce to a very good accuracy the symmetry energy coefficient for medium as well as heavy nuclei. Especially for values of J and L in the region $34^{+0.2}_{-0.2}$ MeV and 65^{+1}_{-1} MeV, respectively, the accuracy is high.

In addition, in Fig. 4(b) we present the mass dependence of the coefficient a_A of several isotopes of Ca, Zr, Sn, and Pb, for two sets of L and J. For a comparison we include also formula (45). The first set ($J = 32$ MeV and $L = 70$ MeV) reproduces on average the binding energies of the corresponding isotopes while the second set ($J = 34$ MeV and $L = 65$ MeV), as we mentioned above, reproduces on average the empirical values of a_A for the isotopes ^{208}Pb, ^{124}Sn, ^{90}Zr, and ^{48}Ca.

In Fig. 5 we compare the allowed pairs of L and J constrained from heavy-ion collisions and nuclear structure observables [10] with those found in the present approach. Actually, the present results lie inside the intersection area suggested by the measurements of the dipole polarizability a_D as well as those found by heavy-ion collisions experiments. However, they lie outside the interval constrained by the nuclear mass measurements, connected with the binding energy, but only for $J < 33$ MeV. This is because constraints between L and J are based on the adjustment of the theoretical to the empirical value of the asymmetry coefficient a_A and not on the corresponding experimental values of the binding energies. It is remarkable that the allowed pairs of L and J consistent with our approach (see the colored lines in Fig. 5) lie at the intersection of the bands originating from other approaches [10].

Figure 6(a) exhibits the dependence of the coefficient a_A on the asymmetry parameter $I = (N - Z)/A$ for various isotopes, for the cases $J = 32$, $L = 70$ and $J = 34$, $L = 65$. In almost all cases there is a soft dependence of a_A on I but, as expected, a strong dependence on the value of J. Similarly, in Fig. 6(b) we indicate the dependence of the neutron skin on the asymmetry parameter I. The most characteristic trend is the occurrence of a strong, linear dependence of $R_{\rm skin}$ on I, that is,

$$R_{\rm skin} = a + bI, \tag{52}$$

where the constants a and b vary in the intervals $-0.02 \leqslant a \leqslant 0.045$ and $1.31 \leqslant b \leqslant 1.45$. Of course, those intervals are strongly dependent on the specific set of values of L and J. For comparison a similar relation suggested in [69] is presented:

$$R_{\rm skin} = (1.01 \pm 0.15)I + (-0.04 \pm 0.03), \tag{53}$$

although in a number of analyzed cases the statistical errors are rather large.

In any case, additional experimental work is necessary to constrain the neutron skin [10]. In particular, the upcoming Lead Radius Experiment II (PREX-II) promises to determine

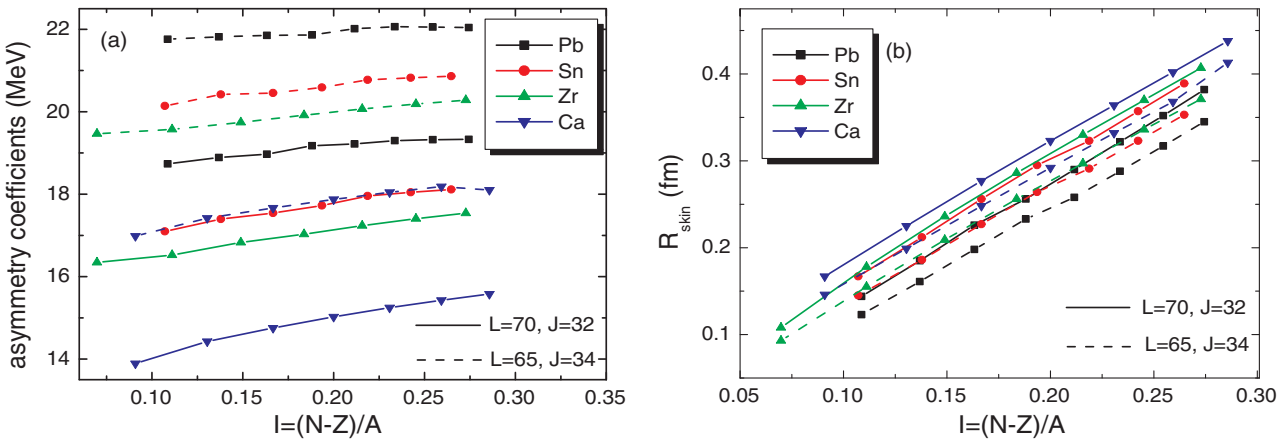

FIG. 6. (Color online) (a) The asymmetry coefficient a_A as a function of the asymmetry parameter I for various isotopes. (b) The corresponding neutron skin $R_{\rm skin}$ dependence on I.

the neutron-skin thickness of ^{208}Pb with a ± 0.06 fm accuracy while the Calcium Radius Experiment (CREX) will provide a high-precision measurement for the neutron radius of ^{48}Ca with an accuracy of ± 0.02 fm [10]. The above measurements will be a very good test for all the theoretical models including the present variational approach.

IV. CONCLUSIONS

In the present work we employ a variational method, in the framework of the Thomas-Fermi approximation, in order to study symmetry energy effects on isovector properties of various neutron-rich nuclei. The key quantity is the asymmetry function $\alpha(r)$ naturally computed by the variational principle. Actually, $\alpha(r)$ is a functional of both the symmetry energy as well as the Coulomb potential, containing the interplay between the long-range Coulomb forces and short-range nuclear ones, and it defines the density distribution of neutrons and protons. All the calculated properties are studied as a function of the slope of the symmetry energy and the value of the symmetry energy at the nuclear saturation density. Since the SE even for low values of nuclear matter is uncertain, the above parametrization is necessary. We find that the neutron skin thickness is very sensitive to L; i.e., it increases rapidly with L. This is expected, at least in the present approximation, since the main ingredient of the relevant calculated integrals, the function $\alpha(r)$, approaches unity very rapidly close to the critical value of r_c (at the surface of the proton distribution). The above characteristic behavior of $\alpha(r)$ is well reflected in the asymmetry coefficient a_A, which is a decreasing function of L. In the case of ^{208}Pb we compare our results with those originating from additional calculations with different models. We conclude that the present approximation supports a stronger sensitivity of the neutron skin thickness on L. However, constraining the total binding energy to be close to the experimental one we see that our results are very close to the mentioned empirical formula.

Our findings from the present study show that experimental knowledge of the symmetry energy at the saturation density J will impose, via the values of the symmetry coefficient a_A, strong constraints on L. More specifically, we note that the set $J = 34$, $L = 65$ reproduces very well the empirical values of a_A corresponding to the nuclei under consideration. In any case, further experimental and theoretical work is necessary for a more detailed exploration of the effects of the symmetry energy on the properties of finite nuclei as well as on neutron star structure.

ACKNOWLEDGMENTS

This work was supported by the Aristotle University of Thessaloniki Research Committee under Contract No. 89286. One of the authors (ChCM) would like to thank P. Ring, G. A. Lalazissis, N. Paar, and C. P. Panos for fruitful discussions.

[1] P. Danielewicz *et al.*, Science **298**, 1592 (2002).
[2] J. M. Lattimer and M. Prakash, Phys. Rep. **442**, 109 (2007).
[3] B. A. Li, L. W. Chen, and C. M. Ko, Phys. Rep. **464**, 113 (2008).
[4] A. W. Steiner, M. Prakash, J. M. Lattimer, and P. J. Ellis, Phys. Rep. **411**, 325 (2005).
[5] J. M. Lattimer, Annu. Rev. Nucl. Part. Sci. **62**, 485 (2012).
[6] D. Vretenar, A. V. Afanasjev, G. A. Lalazissis, and P. Ring, Phys. Rep. **409**, 101 (2005).
[7] F. Sammarruca, Int. J. Mod. Phys. E **22**, 1330031 (2013).
[8] G. Giuliani, H. Zheng, and A. Bonasera, Prog. Part. Nucl. Phys. **76**, 116 (2014).
[9] P. Haensel, A. Y. Potekhin, and D. G. Yakovlev, *Neutron Stars I: Equation of State and Structure* (Springer-Verlag, New York, 2007).
[10] C. J. Horowitz, E. F. Brown, Y. Kim, W. G. Lynch, R. Michaels, A. Ono, J. Piekarewicz, M. B. Tsang, and H. H. Wolter, arXiv:1401.5839 [nucl-th].
[11] P. Danielewicz, Nucl. Phys. A **727**, 233 (2003).
[12] P. Danielewicz and J. Lee, Nucl. Phys. A **818**, 36 (2009).
[13] P. Danielewicz and J. Lee, Nucl. Phys. A **922**, 1 (2014).
[14] J. M. Lattimer and Y. Lim, Astrophys. J. **771**, 51 (2013).
[15] P. Möller, W. D. Myers, H. Sagawa, and S. Yoshida, Phys. Rev. Lett. **108**, 052501 (2012).
[16] A. Ono, P. Danielewicz, W. A. Friedman, W. G. Lynch, and M. B. Tsang, Phys. Rev. C **68**, 051601 (2003).
[17] B. A. Brown, Phys. Rev. Lett. **85**, 5296 (2000).
[18] S. Typel and B. A. Brown, Phys. Rev. C **64**, 027302 (2001).
[19] M. Centelles, P. Schuck, and X. Viñas, Ann. Phys. (NY) **322**, 363 (2007).
[20] M. Centelles, X. Roca-Maza, X. Viñas, and M. Warda, Phys. Rev. Lett. **102**, 122502 (2009).
[21] M. Centelles, S. K. Patra, X. Roca-Maza, B. K. Sharma, P. D. Stevenso, and X. Viñas, J. Phys. G: Nucl. Part. Phys. **37**, 075107 (2010).
[22] M. Warda, X. Viñas, X. Roca-Maza, and M. Centelles, Phys. Rev. C **80**, 024316 (2009).
[23] X. Viñas, M. Centelles, X. Roca-Maza, and M. Warda, Eur. Phys. J. A **50**, 27 (2014).
[24] L. W. Chen, C. M. Ko, and B. A. Li, Phys. Rev. C **72**, 064309 (2005).
[25] R. J. Furnstahl, Nucl. Phys. A **706**, 85 (2002).
[26] H. Kanzawa, M. Takano, K. Oyamatsu, and K. Sumiyoshi, Progr. Theor. Phys. **122**, 673 (2009).
[27] K. Oyamatsu and K. Iida, Phys. Rev. C **75**, 015801 (2007).
[28] F. Sammarruca and P. Liu, Phys. Rev. C **79**, 057301 (2009).
[29] B. K. Agrawal, Phys. Rev. C **81**, 034323 (2010).
[30] B. K. Agrawal, J. N. De, and S. K. Samaddar, Phys. Rev. Lett. **109**, 262501 (2012).
[31] L. W. Chen, Phys. Rev. C **83**, 044308 (2011).
[32] H. Mei, Y. Huang, J. M. Yao, and H. Chen, J. Phys. G: Nucl. Part. Phys. **39**, 015107 (2012).
[33] J. Liu, Z. Ren, C. Xu, and R. Xu, Phys. Rev. C **88**, 024324 (2013).
[34] F. J. Fattoyev and J. Piekarewicz, Phys. Rev. C **86**, 015802 (2012).
[35] F. J. Fattoyev and J. Piekarewicz, Phys. Rev. Lett. **111**, 162501 (2013).
[36] Z. Zhang and L. W. Chen, Phys. Lett. B **726**, 234 (2013).
[37] M. Kortelainen, J. Erler, W. Nazarewicz, N. Birge, Y. Gao, and E. Olsen, Phys. Rev. C **88**, 031305(R) (2013).
[38] S. K. Singh, S. K. Biswal, M. Bhuyan, and S. K. Patra, J. Phys. G: Nucl. Part. Phys. **41**, 055201 (2014).

[39] X. Roca-Maza, M. Brenna, G. Colò, M. Centelles, X. Viñas, B. K. Agrawal, N. Paar, D. Vretenar, and J. Piekarewicz, Phys. Rev. C **88**, 024316 (2013).
[40] A. Z. Mekjian and L. Zamick, Phys. Rev. C **85**, 057303 (2012).
[41] A. R. Bodmer and Q. N. Usmani, Phys. Rev. C **67**, 034305 (2003).
[42] V. Yu. Denisov and V. A. Nesterov, Phys. At. Nucl. **65**, 814 (2002).
[43] V. Prassa, T. Gaitanos, G. Ferini, M. di Toro, G. A. Lalazissis, and H. H. Wolter, Nucl. Phys. A **832**, 88 (2010).
[44] H. H. Wolter, V. Prassa, G. Lalazissis, T. Gaitanos, G. Ferini, M. Di Toro, and V. Greco, Prog. Part. Nucl. Phys. **62**, 402 (2009).
[45] M. K. Gaidarov, A. N. Antonov, P. Sarriguren, and E. Moya de Guerra, Phys. Rev. C **84**, 034316 (2011).
[46] M. K. Gaidarov, A. N. Antonov, P. Sarriguren, and E. Moya de Guerra, Phys. Rev. C **85**, 064319 (2012).
[47] P.-G. Reinhard and W. Nazarewicz, Phys. Rev. C **81**, 051303(R) (2010).
[48] B. K. Sharma and S. Pal, Phys. Lett. B **682**, 23 (2009).
[49] J. P. Blocki, A. G. Magner, P. Ring, and A. A. Vlasenko, Phys. Rev. C **87**, 044304 (2013).
[50] J. Erler, C. J. Horowitz, W. Nazarewicz, M. Rafalski, and P.-G. Reinhard, Phys. Rev. C **87**, 044320 (2013).
[51] Ch. C. Moustakidis, Phys. Rev. C **76**, 025805 (2007).
[52] Ch. C. Moustakidis, Phys. Rev. C **86**, 015801 (2012).
[53] V. P. Psonis, Ch. C. Moustakidis, and S. E. Massen, Mod. Phys. Lett. A **22**, 1233 (2007).
[54] X. Fan, J. Dong, and W. Zuo, Phys. Rev. C **89**, 017305 (2014).
[55] T. Inakura, T. Nakatsukasa, and K. Yabana, Phys. Rev. C **88**, 051305(R) (2013).
[56] M. D. Cozma, Y. Leifels, W. Trautmann, Q. Li, and P. Russotto, Phys. Rev. C **88**, 044912 (2013).
[57] F. J. Fattoyev, J. Carvajal, W. G. Newton, and B. A. Li, Phys. Rev. C **87**, 015806 (2013).
[58] S. Mallik and G. Chaudhuri, Phys. Rev. C **87**, 011602(R) (2013).
[59] C. Xu and Z. Ren, Nucl. Phys. A **913**, 236 (2013).
[60] A. W. Steiner and S. Gandolfi, Phys. Rev. Lett. **108**, 081102 (2012).
[61] S. R. Souza, M. B. Tsang, B. V. Carlson, R. Donangelo, W. G. Lynch, and A. W. Steiner, Phys. Rev. C **80**, 041602(R) (2009).
[62] C. Drischler, V. Soma, and A. Schwenk, Phys. Rev. C **89**, 025806 (2014).
[63] M. B. Tsang, Y. Zhang, P. Danielewicz, M. Famiano, Z. Li, W. G. Lynch, and A. W. Steiner, Phys. Rev. Lett. **102**, 122701 (2009).
[64] M. B. Tsang *et al.*, Phys. Rev. C **86**, 015803 (2012).
[65] A. Klimkiewicz *et al.*, Phys. Rev. C **76**, 051603(R) (2007).
[66] S. Abrahamyan *et al.*, Phys. Rev. Lett. **108**, 112502 (2012).
[67] C. Horowitz *et al.*, Phys. Rev. C **85**, 032501 (2012).
[68] C. M. Tarbert *et al.*, Phys. Rev. Lett. **112**, 242502 (2014).
[69] A. Trzcińska, J. Jastrzębski, P. Lubiński, F. J. Hartmann, R. Schmidt, T. von Egidy, and B. Klos, Phys. Rev. Lett. **87**, 082501 (2001).
[70] D. V. Shetty, S. J. Yennello, A. S. Botvina, G. A. Souliotis, M. Jandel, E. Bell, A. Keksis, S. Soisson, B. Stein, and J. Iglio, Phys. Rev. C **70**, 011601(R) (2004).
[71] D. V. Shetty, S. J. Yennello, and G. A. Souliotis, Phys. Rev. C **75**, 034602 (2007).
[72] P. Marini *et al.*, Phys. Rev. C **87**, 024603 (2013).
[73] M. Veselský and Y. G. Ma, Phys. Rev. C **87**, 034615 (2013).
[74] H. Bethe, Phys. Rev. **167**, 879 (1968).
[75] P. Ring and P. Schuck, *The Nuclear Many-Body Problem* (Springer, Heidelberg, 1980).
[76] W. D. Myers and W. J. Swiatecki, Ann. Phys. (NY) **84**, 186 (1974).
[77] M. Baldo, L. M. Robledo, P. Schuck, and X. Viñas, Phys. Rev. C **87**, 064305 (2013).
[78] T. Niksic, D. Vretenar, and P. Ring, Progr. Part. Nucl. Phys. **66**, 519 (2011).
[79] K. A. Brueckner, J. R. Buchler, S. Jorna, and R. J. Lombard, Phys. Rev. **171**, 1188 (1968).
[80] K. A. Brueckner, J. R. Buchler, R. C. Clark, and R. J. Lombard, Phys. Rev. **181**, 1543 (1969).
[81] K. A. Brueckner, J. H. Chirico, and H. W. Melder, Phys. Rev. C **4**, 732 (1971).
[82] J. R. Buchler and Z. Barkat, Phys. Rev. Lett. **27**, 48 (1971).
[83] R. J. Lombard, Ann. Phys. **77**, 380 (1973).
[84] W. D. Myers and W. J. Świątecki, Phys. Rev. C **57**, 3020 (1998).
[85] R. W. Hasse and W. D. Myers, *Geometrical Relationships of Macroscopic Nuclear Physics* (Springer-Verlag, Berlin, 1988).
[86] M. Baldo, L. Robledo, P. Schuck, and X. Viñas, J. Phys. G: Nucl. Part. Phys. **37**, 064015 (2010).